Non-aromatic carbonaceous species formed in the circumstellar environments of evolved stars

Lidia Martínez[1+], Gonzalo Santoro[1+], Pablo Merino[1,2+], Mario Accolla[1], Koen Lauwaet[3], Jesús Sobrado[4], Hassan Sabbah[5], Ramón J. Pelaez[6], Victor J. Herrero[6], Isabel Tanarro[6], Marcelino Agúndez[2], Alberto Martín[2], Roberto Otero[2], Gary J. Ellis[7], Christine Joblin[5]*, José Cernicharo[2]* and José A. Martín-Gago[1]*

[1]Instituto de Ciencia de Materiales de Madrid (ICMM. CSIC). Materials Science Factory. Structure of Nanoscopic Systems Group. C/ Sor Juana Inés de la Cruz 3, 28049 Cantoblanco, Madrid, Spain.

[2]Instituto de Física Fundamental (IFF. CSIC). Group of Molecular Astrophysics, C/ Serrano 123, 28006 Madrid, Spain

[3]IMDEA Nanociencia, Ciudad Universitaria de Cantoblanco, 28049 Cantoblanco, Madrid, Spain

[4]Centro de Astrobiología (CAB, INTA-CSIC). Crta- de Torrejon a Ajalvir km4, 28850, Torrejon de Ardoz, Madrid, Spain.

[5]IRAP, Université de Toulouse, CNRS, CNES, 9 Av. du Colonel Roche, 31028 Toulouse Cedex 4, France

[6]Instituto de Estructura de la Materia. CSIC. Molecular Physics Department. C/Serrano 123, 28006 Madrid, Spain.

[7]Instituto de Ciencia y Tecnología de Polímeros (ICTP. CSIC). C/ Juan de la Cierva 3, 28006-Madrid, Spain.

+. Equally contributed

*Corresponding authors: gago@icmm.csic.es, jose.cernicharo@csic.es, christine.joblin@irap.omp.eu

Stars, like our Sun, in their final stages of evolution reach the asymptotic giant branch (AGB) accompanied by a massive ejection of matter containing the vast chemical complexity that provides the building blocks of planets and life[1,2]. From observations of prototype carbon-rich AGBs a large number of organic species[3–5] have been discovered that are some of the basic ingredients of cosmic dust in the circumstellar envelope (CSE). However, the chemical nature of cosmic carbon and its role in the formation of small molecules is still controversial. Polycyclic aromatic hydrocarbons (PAHs) are widespread in regions of massive star formation, identified by the emission of aromatic infrared bands (AIBs)[6], but a robust explanation of how they form is still lacking, especially in evolved AGB stars where AIBs are only detected at late stages when the star emits ultraviolet (UV) radiation[7]. Laboratory-based experiments are indispensable to elucidate the nature of cosmic dust[8–12], but most rely on uncontrolled combustion or decomposition of molecular precursors under conditions very unlike those in evolved star photospheres. In this letter, using an unprecedented experimental setup[13] we investigate the basic chemistry operating in CSE to produce clusters and dust using exclusively gas-phase C atoms and molecular hydrogen. We show that gas-phase aggregation of C atoms in a molecular hydrogen atmosphere leads to the highly efficient formation of carbon nanoparticles, carbon clusters and aliphatic C, with no evidence for aromatics, which can be formed by additional processing of aliphatics on C-dust grains.

Our experimental set-up, *Stardust*[13] presents several advantages, in particular its versatility for the design of experiments that combine highly controlled UHV technology with *in-situ* characterization techniques, the latter being mandatory because of the high reactivity expected of the formed carbon nanostructures to atmospheric and residual gases[14]. A simplified block diagram of *Stardust* is shown in Fig. 1a and a technical description is given in Supplementary Information 1 and Supplementary Fig. 1. The working principle is the vaporization of C atoms from a graphite target with a sputter gas aggregation source, using Ar as the sputtering gas. This step is followed by injection of the most abundant gas species in AGB environments, H_2. The vaporized C atoms react with H_2 and are subsequently dragged through a nozzle by differential pressure into the next chambers where they are collected on inert Au surfaces for further analysis. Once the carbonaceous cosmic-dust analogue passes the nozzle of the first chamber, no further growth takes place. The composition of the small, gas-phase species is analysed by mass spectrometry (MS) before sample collection at position QMS in fig. 1a. Finally, the deposit is characterized *in situ* in a third chamber by Thermal Programmed Desorption (TPD).

Unlike previous experiments, our approach starts with atoms to produce nanoparticles, C-clusters and hydrocarbons, without the requirement for C-bearing molecular precursors, as is expected to occur in the atmospheres of AGB stars. The initial gas-phase vaporized C atoms may interact with residual or injected molecular hydrogen at different densities, and there are no other species involved except Ar. The vaporized C atoms have a density of about 2.5×10^{10} atoms·cm^{-3}. Albeit some orders of magnitude higher than that estimated for the dust nucleation zone of stars[15], it provides an effective method to accelerate the chemistry, which takes years in a real AGB envelope. Regarding the hydrogen, two cases are considered: low and high densities. In the first case, H_2 molecules are in the same proportion as C atoms, which can be achieved either using residual hydrogen or by introducing very low H_2 densities that are

estimated in the range of $1.5x10^{10}$ mol·cm^{-3}; a value typically accepted for the dust nucleation zone at distances from the star of around 10^{14} cm [15]. In the second case, a high H_2 density is achieved by introducing extra hydrogen at a concentration estimated at $1.5x10^{12}$ mol·cm^{-3}, two orders of magnitude higher than that of vaporized C atoms. This situation provides a more appropriate simulation of the chemistry in CSE in terms of H_2/C abundance (~3000 [16]).

Fig. 1b shows a typical Atomic Force Microscope (AFM) image obtained of the C-dust collected on a SiOx surface at position QMS, where two different morphological features can be identified. Firstly, C-nanograins (encircled in white in Fig. 1b) are efficiently produced as the most abundant constituents, with a surface density that increases with deposition time. These spherical grains exhibit an extremely narrow size distribution with an average size of 9 nm, corresponding to > 10^5 C atoms. Although larger grains (typically 100 nm) are thought to be present in space, in *Stardust* the nanoparticle size is conditioned by geometry and experimental parameters and can be considered to represent the initial stages of carbonaceous dust formation and growth.

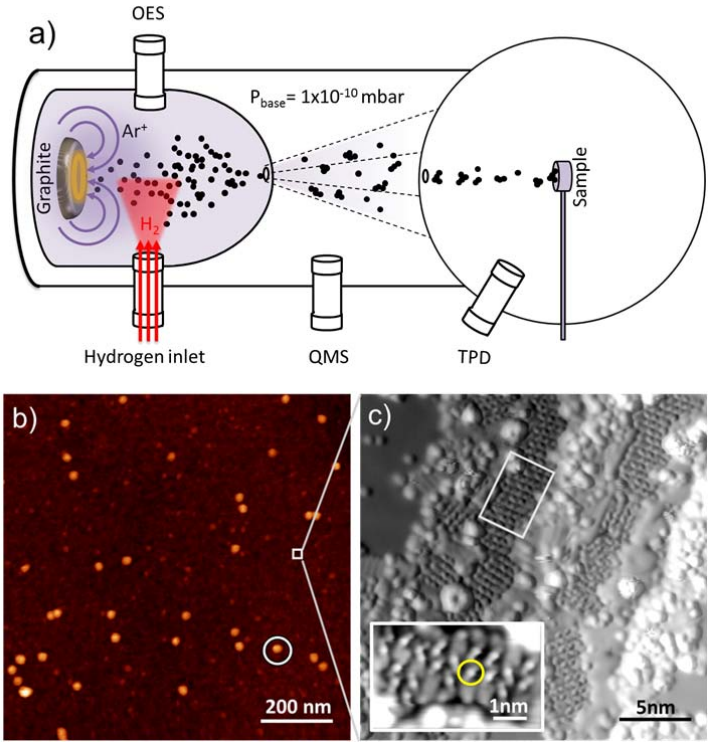

Fig. 1 | Production and structure of cosmic dust analogues. a, Schematic of the main components of the *Stardust* machine: aggregation zone (violet), expansion area where the quadrupole mass spectrometer (QMS) is installed, and analysis area, where thermal programmed desorption (TPD) is located. **b**, AFM image showing the presence of C-nanoparticles and small clusters forming a continuous layer. A single nanoparticle is encircled. **c**, STM image of a C-cluster film deposited on a metal surface. Scanned area: 25x25 nm^2, recorded at 50 pA, 1400 mV. Inset: Zoom of the rectangular area 5x3 nm^2, I= 10 pA, V=1400 mV. A small molecule is encircled.

The other principal constituent of the C-dust analogues can be located on the flat regions of Fig. 1b, where a thin mantle of material is observed, for instance in the area marked by a white square (see Supplementary Figure 2). Structural resolution of these zones cannot be achieved using standard AFM, and more powerful *in situ* microscopies are required. Fig. 1c shows a scanning tunnelling microscope (STM) image obtained from the C analogues deposited on a Au surface. This image shows that the material is made up of a collection of individual structures no larger than 1 nm in width and with a maximum apparent height of 1 nm. The small size of these structures, such as that encircled in the inset of Fig. 1c, suggests that they correspond to individual molecules that typically comprise 3 – 5 C atoms. Some of these small molecules can self-assemble on the surface forming 2D islands, such as the region marked within a rectangle, magnified in the inset and in Supplementary Figure 3. This is a surface-mediated process suggesting electrostatic interactions between the molecules upon absorption on surfaces.

To further understand the nature of these carbon analogues we used gas-phase analysis techniques. Optical emission spectra (OES) were recorded at the OES position indicated in Fig. 1a. The Swan C_2 lines are observed in Fig. 2a in the presence of low H_2 density, but are not found in the case of higher H_2 density. On the contrary, the H_α emission line is only observed at high H_2 density. These observations suggest that excited H atoms are generated during the chemical evolution, involving $C_2 + H_2 \rightarrow CCH + H$. The absence of the C_2 lines at high H_2 density indicates that most of the excited C_2 formed is consumed in this reaction. Interestingly, C_2 and H species are only detected in the regions close to the magnetron, which compares very well to observations from the photosphere of evolved stars where some H has been found and C_2 bands are prominent[17].

Fig. 2b presents the evolution of the masses of some relevant species during the experiment recorded at position QMS of Fig. 1a. For low H_2 concentration, a peak at 26 amu mainly corresponding to C_2H_2 was detected along with fragments of C_2H_4, C_2H_6 and larger aliphatic molecules. A peak at 16 amu is also observed, corresponding to methane. In the case of high H_2 densities we also detect an increase in the main ionization fragments of ethane (C_2H_6), ethylene (C_2H_4), propane (C_3H_8) and larger alkanes. Importantly, here these species were formed directly from C atoms and molecular hydrogen, without introducing them as precursors, using ratios and aggregation processes similar to those reported to take place in CSE [16,18]. Fig. 2b shows a decrease in the partial pressure of H_2 when C evaporation is initiated, suggesting that H_2 is partially consumed by chemical reactions that occur in the aggregation zone. It is important to remark that neither benzene (C_6H_6) nor toluene (C_7H_8) are detected in in the MS measurements (Supplementary Figure 4).

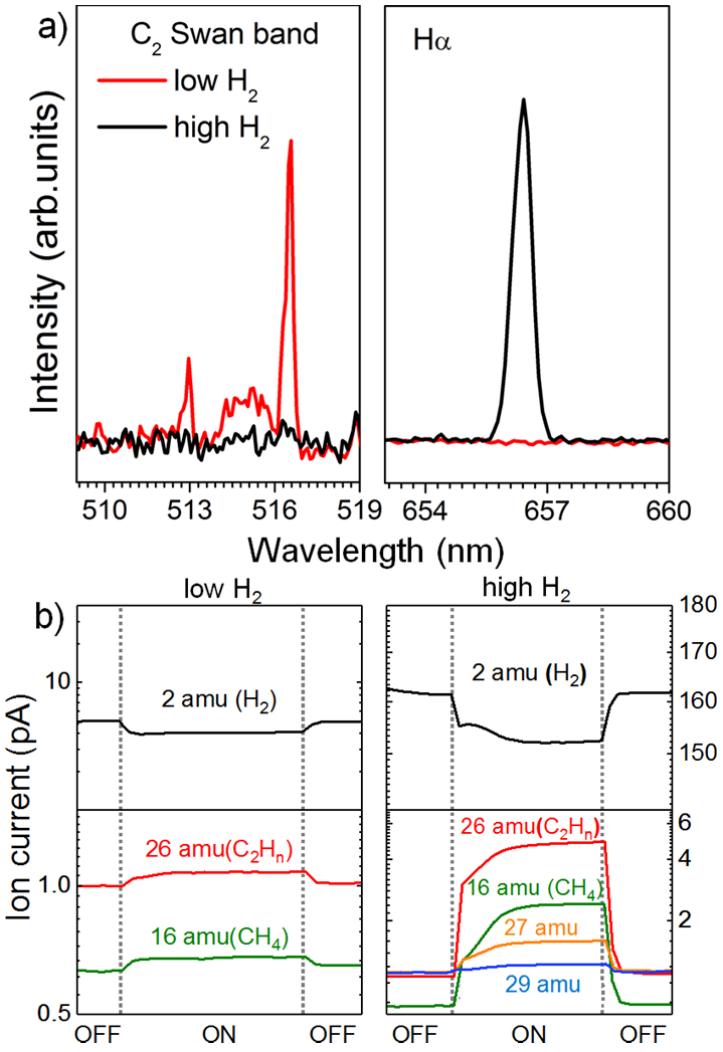

Fig. 2 | Gas phase characterization. **a,** Optical emission spectra recorded at position OES in Fig. 1a for low and high H_2 densities. **b,** *In situ* gas-phase detection at position QMS of masses 2, 16, 26, 27 and 29 (amu) for low and high H_2 densities. Dashed lines indicate the time period where the magnetron was switched on and off.

Additionally, we have used *ex situ* laser desorption ionization (LDI) mass-spectrometry in the so-called set-up *AROMA*[19], a machine with high sensitivity for PAH detection. Fig. 3 provides the ion distribution obtained by desorption/ionization of representative samples grown with both H_2 densities, showing that the molecular species generated have < 20 carbon atoms. Above 300 amu the signal completely vanishes, showing that no traces of fullerenes could be detected (see Supplementary Figure 5). Pure carbon clusters are observed from C_8^+ to C_{19}^+, and above C_9^+ these are poorly hydrogenated, which can be understood by the formation of close-cage structures with reduced dimensionality and, thus, lower reactivity[20]. We have found no evidence of formation of C_{60}. C-clusters with a low degree of hydrogenation are observed for species containing 4 to 9 C atoms, which are discussed in Supplementary 5.

The results from LDI-MS (see Supplementary Fig. 5) are summarized in Fig.3 with double bond equivalent (DBE) bar-graphs where the species generated are classified in families. The analysis suggests a higher abundance of HC clusters when low H_2 density is used, suggesting the presence of the more saturated aliphatic species at high H_2 density, not found by LDI-MS but evidenced by QMS (Fig. 2). Masses corresponding to benzene or toluene, as key aromatic species, are not (or only very marginally) detected, neither in the LDI-MS analysis (Fig. 3) or the QMS measurements (see Supplementary Fig. 4). A few larger aromatic species, up to $C_{16}H_{10}$, are detected to a maximum of 3% for both H_2 densities. Therefore, it appears that the chemistry involved in the CSE does not favour the formation of PAHs, whose abundance can reach up to 18% of the total carbon species in the ISM[21].

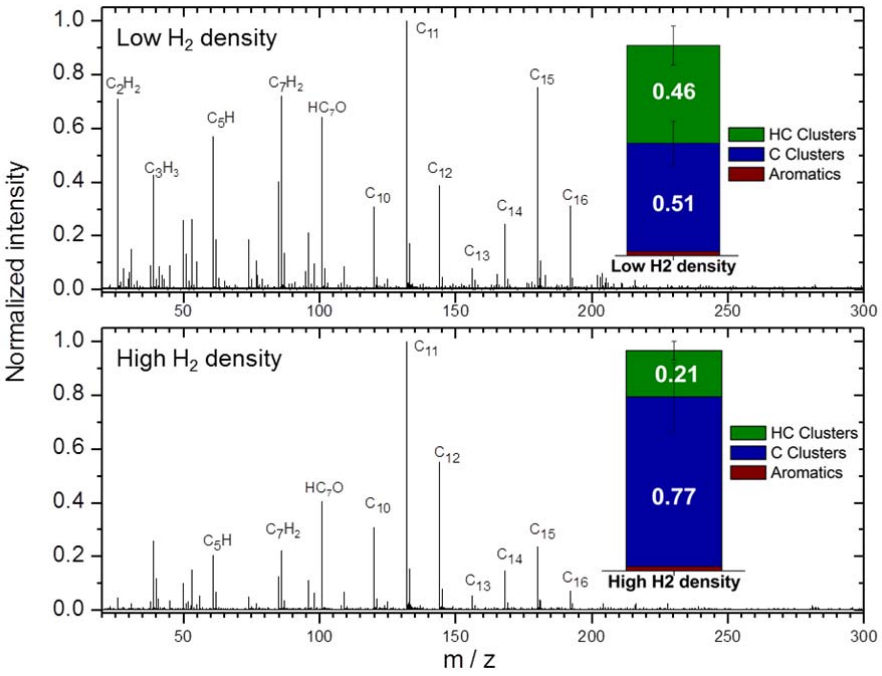

Fig. 3 | *Ex situ* laser desorption/ionization (LDI) mass-spectrometry from samples grown with a low (upper panel) and high (lower panel) H_2 densities. Insets: Stacked bar graphs summarizing the family compositions by double bond equivalent (DBE) analysis. The error bars correspond to the relative standard deviation obtained for the total ion signal over a mass range for each family of compounds.

Consequently, considering the MS results in Fig. 2b and Fig. 3, we can outline several aspects of the chemistry involved. Time-dependent chemical kinetics models (see Supplementary 6) to compute the evolution of the chemical composition of the gas mixture in *Stardust* show, assuming that most of the carbon from the magnetron is atomic, that the following three-body reactions initiate the chemistry: C+C+Ar and C+H_2+Ar leading to C_2 and CH_2 species, respectively. The kinetic simulations provide clear routes to the formation, via neutral reactions, of the molecular species detected in Fig. 2b (CH_4, C_2H_2, C_2H_4, C_2H_6 and C_3H_8),

provided that the reacting species persist for sufficient time in the magnetron zone. This condition can be fulfilled in this type of magnetron where material has been reported to remain trapped[22] (see Supplementary for further discussion).

Fig. 4 shows a representative MS single scan at 430K from an *in situ* TPD experiment (see complete graph in Supplementary Figure 7). Albeit a precise assignment of masses is difficult to perform, families of C_nH_m hydrocarbons can be identified. The most abundant masses of 26 amu, 39 amu and 41 amu, all belong to known fragments of larger aliphatic hydrocarbons[23]. Interestingly, in our experiment benzene and naphthalene were observed after annealing the deposited carbon above 355K. These aromatic species are most likely formed after a catalytic recombination of small hydrocarbons on the gold surface, a process reported in surface chemistry[24,25], since they were not observed in the LDI-MS analysis which is highly sensitive to aromatics. The fact that aromatics could be formed after annealing of carbonaceous aliphatics deposited on a C-rich surface needs to be further explored as a possible mechanism for the formation of these species in warm CSE environments. Indeed, AIBs, the signature for PAHs, are not convincingly detected in AGBs but are observed at later stages when the star emits ultraviolet (UV) radiation and process the Carbon-dust[7].

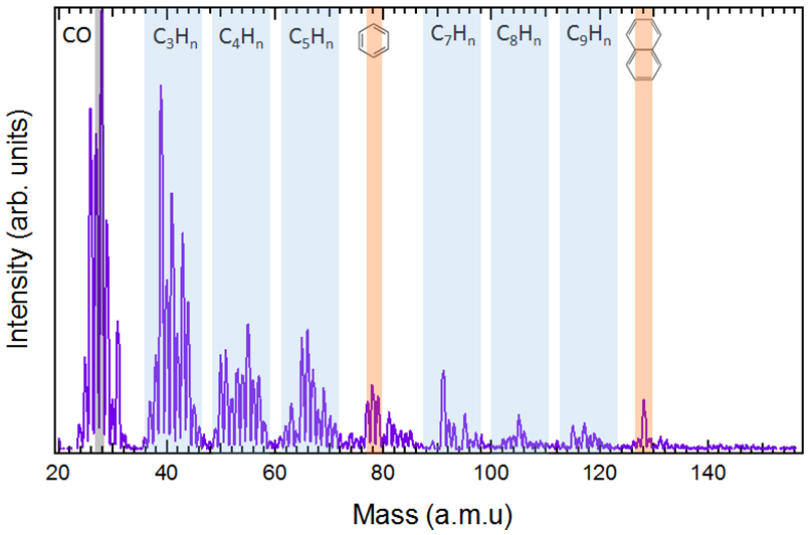

Fig. 4 | Representative scan from a TPD experiment on C-analogues formed with high H_2 density on a Au surface.

The combination of laboratory astrochemistry, surface science and astronomical observations can unveil the chemical routes that operate in the envelope of evolved stars, providing new insights into the chemistry of carbonaceous stardust formation. There are several models to account for the presence of aromatic species in CSE; one involves the polymerization of acetylene to benzene[5] and further growth by the hydrogen abstraction acetylene addition (HACA) mechanism[26,27]. Other scenarios involve the processing of SiC dust grains[28] or the catalytic activity of C_2H_2 on silicate surfaces[29]. Our results suggest that PAHs are not efficiently

198 formed during gas-phase growth in CSE, which we show to generate aliphatic material and C-
199 clusters together with amorphous carbon grains. However, the species that are deposited on
200 dust grains are susceptible to further processing and can auto-catalyse to form aromatic
201 species upon thermal activation, which could be provided as a result of the significant rise in
202 dust temperature that occurs in highly UV-irradiated environments.

203

Methods

Fabrication of the dust analogues. The carbon dust analogues were fabricated using a scaled-up MICS working under UHV conditions (base pressure $1x10^{-9}$ mbar). The magnetrons were loaded with a graphite target of 99.95% purity. The Ar flux used for the experiments was 150 sccm. The typical power applied to the magnetron was 100 W and the working aggregation length (distance between the magnetron and the exit nozzle) was 374 mm.

Extra-pure H_2 (99.99% purity) was injected during fabrication through one of the lateral entrances of the aggregation zone of the MICS (see Supplementary Figure 1). The doses used for these experiments were: 0, $4x10^{-4}$ and 1 sccm, with an Ar flux maintained at 150 sccm. The substrates employed for collecting the NPs are boron-doped Si(100) with its native oxide for AFM; polycrystalline Au for *AROMA* experiments; Au(111) for TPD analysis.

Atomic Force Microscopy (AFM) measurements were performed in the dynamic mode using a Cervantes AFM System equipped with the *Dulcinea* electronics from Nanotec Electronica S.L. All images were analyzed using WSxM software[30].

Scanning tunneling microscopy (STM). Samples for scanning tunnelling microscopy (STM) were prepared in *Stardust* and transferred without exposing the samples to the atmosphere to the STM chamber, located in a different laboratory, using a UHV suitcase with an ion-getter pump (base pressure $<1x10^{-9}$ mbar) to avoid chemical reaction with environmental gases[14]. Samples are deposited on an atomically flat single crystal Au(111) surface pre-cleaned by repeated sputtering/annealing cycles, which consisted of sputtering for 10 min using Ar^+ ions at an energy of 1.25 kV and subsequent annealing at 800 K for 5 min. Clean Au(111) is later exposed to the carbon analogues for 5 minutes keeping the sample at room temperature, then immediately transferred to the UHV suitcase and to the STM chamber. The total time between sample growth and insertion in the STM cryostat was limited only by the pumping of the load lock volume. STM measurements were performed at 4K in a LT-STM (Scienta Omicron) with a base pressure $<10^{-11}$ mbar.

Optical emission spectroscopy (OES). The light emitted by the plasma generated in front of the magnetron was collected through a fused silica window and an optical fibre of fused silica, and analysed by OES (see position in Fig. 1a) using a 193 mm focal length, motorized Czerny-Turner spectrograph (Andor, model Shamrock SR-193-i-A) equipped with a CCD camera (iDus DU420A-BVF). Two diffraction gratings with 1200 grooves/mm and 1800 grooves/mm, installed in a movable turret, provide spectral ranges of 300-1200 nm and 200-950 nm, respectively, and nominal spectral resolutions of 0.22 nm and 0.15 nm, respectively (for an input slit width of 20 µm). The relative spectral efficiencies of the all the spectroscopic equipment was quantified for both diffraction gratings with a calibrated tungsten lamp.

***In situ* mass spectrometry (MS).** The gaseous species produced during the fabrication of the C-dust analogues were detected *in situ* with a quadrupole mass spectrometer (QMS) (0-100 amu).

Laser desorption/ionization (LDI) mass-spectrometry: the *AROMA* machine. *AROMA* (Aromatic Research of Organics with Molecular Analyzer) is dedicated to the analysis, with

micron-scale resolution, of the carbonaceous molecular content of cosmic dust analogues. The experimental setup consists of a microprobe laser desorption ionization chamber and a segmented linear quadrupole ion trap connected to an orthogonal time of flight mass spectrometer (LQIT-oTOF). For each detected m/z peak with a signal-to-noise ratio (S/N) greater than 10, a chemical formula was assigned using the mMass software[31], an open source mass spectrometry tool. The double bond equivalent (DBE) for each molecular formula was then calculated using the following equation for a given chemical formula of hydrocarbon species C_cH_h: DBE = c-(h/2)+1. This method allows sorting of the detected ions into families of compounds[32]. This is done using empirical factors that delineate DBE boundaries in complex natural organic matter[33]. Hydrocarbons with 0.5 < DBE/C < 0.9 are considered to be aromatics. The line DBE/C ~1 corresponds to C clusters and the species falling in the zone 0.9≤DBE/C<1 are referred to as HC clusters, which includes C_cH_2 polyynes. Once all the detected species were sorted, the ion signal percentage was calculated for each family by dividing the sum of peak intensities detected in each family by the total ion intensity.

Thermal Programmed Desorption (TPD). Experiments were performed *in-situ* to determine the mass spectra of the carbon analogues deposited on low reactivity surfaces annealed at increasing temperatures. TPD was performed using a Pfeiffer HiQuad QMG 700 with QMA 400 mass spectrometer with a CP 400 ion counter preamplifier. The instrumentation permits measurement of masses between 0 and 512 amu with a detection limit of 10^{-15} mbar. After carbon analogue deposition the samples were placed in front of the quadrapole at a short distance (>1 cm) ensuring that the majority of the collected gas species derive from the surface of the sample surface. Atomically flat Au(111) and HOPG substrates were used in the experiments, yielding comparable TPD spectra, which precludes significant on-surface chemistry during the annealing process. Au(111) surfaces were cleaned *in-situ* by the standard methodology of sputtering/annealing. HOPG was mechanically cleaved *ex-situ* and consecutively introduced into the vacuum system, which ensures an atomically fresh graphite surface prior to deposition. The carbon analogues were deposited during 100 minutes. This amount of carbon material ensures there is enough to obtain well-defined signals in the TPD experiments. A temperature ramp of 12.5°C·min^{-1} was applied from room temperature to the maximum temperature examined (400 °C).

Acknowledgements. We thank the European Research Council for funding support under Synergy Grant ERC-2013-SyG, G.A. 610256 (NANOCOSMOS). Also, partial support from the Spanish Research Agency (AEI) through grants MAT2017-85089-c2-1R, FIS2016-77578-R and FIS2016-77726-C3-1-P is acknowledged. Support from the FotoArt-CM Project (P2018/NMT-4367) through the Program of R&D activities between research groups in Technologies 2013, co-financed by European Structural Funds, is also recognised.

Author contributions. *In-situ* experiments in *Stardust* were performed by L.M, G.S, P.M, and M.A.; C.J. and H.S. performed LDI experiments. P.M.; K.L, R.O and A.M performed STM images. L.M. performed AFM images. RJ.P, V.J.H. and I.T. performed the OES experiments. M.A. made the kinetic calculations. G.J.E. and J.A.M-G wrote the first version of the manuscript. J.A.M-G supervised *in-situ* experiments, and C.J. and J.C the astrochemical interpretation. All authors discussed and contributed to the final version of the manuscript.

Competing interests. The authors declare no competing interests.

Additional information. Additional text, figures and references are provided.

REFERENCES

1. Kwok, S. The synthesis of organic and inorganic compounds in evolved stars. *Nature* **430,** 985–991 (2004).

2. Henning, T. & Salama, F. Carbon in the Universe. *Science* **282,** 2204–2210 (1998).

3. Fonfria, J. P., Cernicharo, J., Richter, M. J. & Lacy, J. H. A Detailed Analysis of the Dust Formation Zone of IRC +10216 Derived from Mid-Infrared Bands of C 2 H 2 and HCN. *Astrophys. J.* **673,** 445–469 (2008).

4. Fonfría, J. P., Agúndez, M., Cernicharo, J., Richter, M. J. & Lacy, J. H. Carbon chemistry in IRC+10216: Infrared detection of diacetylene. *Astrophys. J.* **852,** 80 (2018).

5. Cernicharo, J. *et al.* Infrared Space Observatory's Discovery of C4H2, C6H2, and Benzene in CRL 618. *Astrophys. J.* **546,** L123–L126 (2001).

6. Peeters, E., Spoon, H. W. W. & Tielens, A. G. G. M. PAHs as a tracer of star formation? *Astrophys. J.* **613,** 986–1003 (2004).

7. Kwok, S. & Zhang, Y. Mixed aromatic-aliphatic organic nanoparticles as carriers of unidentified infrared emission features. *Nature* **479,** 80–83 (2011).

8. Kroto, H. W., Heath, J. R., O'Brien, S. C., Curl, R. F. & Smalley, R. E. C60: Buckminsterfullerene. *Nature* **318,** 162–163 (1985).

9. Jäger, C., Huisken, F., Mutschke, H., Jansa, I. L. & Henning, T. Formation of polycyclic aromatic hydrocarbons and carbonaceous solids in gas-phase condensation experiments. *Astrophys. J.* **696,** 706–712 (2009).

10. Pino, T. *et al.* The 6.2 um band position in laboratory and astrophysical spectra: a tracer of the aliphatic to aromatic evolution of interstellar carbonaceous dust. *Astron. Astrophys.* **490,** 665–672 (2008).

11. Contreras, C. S. & Salama, F. LABORATORY INVESTIGATIONS OF POLYCYCLIC AROMATIC HYDROCARBON FORMATION AND DESTRUCTION IN THE CIRCUMSTELLAR OUTFLOWS OF CARBON STARS. *Astrophys. J. Suppl. Ser.* **208,** 6 (2013).

12. Peláez, R. J. *et al.* Plasma generation and processing of interstellar carbonaceous dust analogs. *Plasma Sources Sci. Technol.* **27,** 035007 (2018).

13. Martínez, L. *et al.* Precisely controlled fabrication, manipulation and in-situ analysis of Cu based nanoparticles. *Sci. Rep.* **8,** (2018).

14. Ravagnan, L. *et al.* Cluster-Beam Deposition and in situ Characterization of Carbyne-Rich Carbon Films. *Phys. Rev. Lett.* **89,** 285506 (2002).

15. Agundez, M. & Cernicharo, J. Oxygen Chemistry in the Circumstellar Envelope of the Carbon-Rich Star IRC +10216. *Astrophys. J.* **650,** 374–393 (2006).

16. Cernicharo, J. The Polymerization of Acetylene, Hydrogen Cyanide, and Carbon Chains in the Neutral Layers of Carbon-rich Proto-planetary Nebulae. *Astrophys. J.* **608,** L41–L44 (2004).

17. Contreras, C. S., Sahai, R., de Paz, A. G. & Goodrich, R. Echelle long-slit optical spectroscopy of evolved stars. *Astrophys. J. Suppl. Ser. Vol. 179, Issue 1, pp. 166-194 (2008).* **179,** 166–194 (2008).

18. Agundez, M. *et al.* The growth of carbon chains in IRC+10216 mapped with ALMA. *Astron. Astrophys.* **601,** A4 (2017).

19. Sabbah, H. *et al.* Identification of PAH Isomeric Structure in Cosmic Dust Analogs: The AROMA Setup. *Astrophys. J.* **843,** 34 (2017).

20. Van Orden, A. & Saykally, R. J. Small Carbon Clusters: Spectroscopy, Structure, and Energetics. *Chem. Rev.* **98,** 2313–2358 (1998).

21. Joblin, C., Leger, A. & Martin, P. Contribution of polycyclic aromatic hydrocarbon molecules to the interstellar extinction curve. *Astrophys. J.* **393,** L79 (1992).

22. Kousal, J. *et al.* Magnetron-sputtered copper nanoparticles: lost in gas aggregation and found by in situ X-ray scattering. *Nanoscale* **10,** 18275–18281 (2018).

23. Atomic Spectra Database | NIST. at <https://www.nist.gov/pml/atomic-spectra-database>

24. Alyabyev, S. B. & Beletskaya, I. P. Gold as a catalyst. Part II. Alkynes in the reactions of carbon–carbon bond formation. *Russ. Chem. Rev.* **87,** 984–1047 (2018).

25. Zaera, F. Surface chemistry of hydrocarbon fragments on transition metals: Towards understanding catalytic processes. *Catalysis Letters* **91,** 1–10 (2003).

26. Frenklach, M. & Feigelson, E. D. Formation of polycyclic aromatic hydrocarbons in circumstellar envelopes. *Astrophys. J.* **341,** 372 (1989).

27. Zhao, L. *et al.* Pyrene synthesis in circumstellar envelopes and its role in the formation of 2D nanostructures. *Nat. Astron.* **2,** 413–419 (2018).

28. Merino, P. *et al.* Graphene etching on SiC grains as a path to interstellar polycyclic aromatic hydrocarbons formation. *Nat. Commun.* **5,** 3054 (2014).

29. Tian, M. *et al.* Catalytic conversion of acetylene to polycyclic aromatic hydrocarbons over particles of pyroxene and alumina. *Philos. Trans. R. Soc. A Math. Phys. Eng. Sci.* **371,** (2013).

30. Horcas, I. *et al.* WSXM: A software for scanning probe microscopy and a tool for nanotechnology. *Rev. Sci. Instrum.* **78,** 013705 (2007).

31. Strohalm, M., Kavan, D., Novák, P., Volný, M. & Havlíček, V. mMass 3: A Cross-Platform Software Environment for Precise Analysis of Mass Spectrometric Data. *Anal. Chem.* **82,** 4648–4651 (2010).

32. Marshall, A. G. & Rodgers, R. P. Petroleomics: Chemistry of the underworld. *Proc. Natl. Acad. Sci.* **105,** 18090–18095 (2008).

33. Koch, B. P. & Dittmar, T. From mass to structure: An aromaticity index for high-resolution mass data of natural organic matter. *Rapid Commun. Mass Spectrom.* **20,**

926–932 (2006).